IEEE Access
Multidisciplinary | Rapid Review | Open Access Journal

Received 12 April 2023, accepted 27 April 2023, date of publication 19 May 2023, date of current version 26 July 2023.

Digital Object Identifier 10.1109/ACCESS.2023.3277955

RESEARCH ARTICLE

Terahertz Women Reproductive Hormones Sensor Using Photonic Crystal Fiber With Behavior Prediction Using Machine Learning

A. NAESHA NITHISH[1], SHOBHIT K. PATEL[2], (Senior Member, IEEE), N. AYYANAR[1], JAYMIT SURVE[3], (Graduate Student Member, IEEE), S. RAJARAM[1], (Senior Member, IEEE), S. N. DEEPA[4], TRUONG KHANG NGUYEN[5], (Senior Member, IEEE), AND FAHAD AHMED AL-ZAHRANI[6]

[1]Department of ECE, Thiagarajar College of Engineering, Madurai, Tamil Nadu 625015, India
[2]Department of Computer Engineering, Marwadi University, Rajkot, Gujarat 360003, India
[3]Department of Electrical Engineering, Faculty of Technology, Marwadi University, Rajkot, Gujarat 360003, India
[4]Department of Electrical Engineering, National Institute of Technology Arunachal Pradesh, Jote, Arunachal Pradesh 791113, India
[5]Faculty of Information Technology, School of Technology, Van Lang University, Ho Chi Minh City 700000, Vietnam
[6]Computer Engineering Department, Umm Al-Qura University, Mecca 24381, Saudi Arabia

Corresponding authors: Truong Khang Nguyen (khang.nt@vlu.edu.vn) and Fahad Ahmed Al-Zahrani (fayzahrani@uqu.edu.sa)

This work was supported by the Deputyship for Research & Innovation, Ministry of Education, Saudi Arabia, under Project IFP22UQU4170008DSR094.

ABSTRACT In this article, we propose a rectangular hollow core Photonic Crystal Fiber (PCF) sensor for high detection of women's reproductive hormones (progesterone and estradiol) in the blood sample at THz regime (0.8 THz to 1.7 THz). The numerical sensing performances are evaluated by the full vector finite element method (FVFEM). We have achieved improved relative sensitivity with minimal loss for sensing progesterone concentrations and estradiol concentrations by optimizing structural parameters. The obtained maximum relative sensitivity is 99.87% for 10 n mol/L (progesterone) and 99.88% for 3 n mol/L (Estradiol) at 1.35 THz. Further, we have obtained low effective material loss (EML) and a large effective mode area. The primary takeaway from this research is that it's critical to monitor estradiol and progesterone levels in order to ensure that a woman's reproductive system is functioning in a balanced manner and in general health systems. Also, this biosensor can be fabricated by current fabrication technologies. Moreover, the prediction carried out with the help of Locally Weighted Linear Regression, and hyperparameter tuning, we can conclude that for weighting hyperparameter value of 0.02. We have achieved the maximum prediction accuracy with the unity R^2 score and this model can be employed for the prediction of relative sensitivity for various parameters.

INDEX TERMS Hollow core PCF, biosensor, progesterone, estradiol, relative sensitivity, locally weighted linear regression.

I. INTRODUCTION

A wide range of sensor technologies have been developed throughout the year for sensing biomolecules [1], [2], [3]. Among these, optical biosensors have made a significant impact on the research for the detection of biomolecules. In the biomedical field, hormones play an important role in the human body. Imbalanced levels of hormones lead to dangerous diseases like cancer, osteoporosis, hyperplasia of the cardiovascular system, etc. [4], [5]. Particularly, progesterone and estradiol hormones connect in each and every cell and tissue of female bodies. Both hormones cooperate and are in charge of the changes that occur during pregnancy. For a woman's reproductive system to function properly and to

The associate editor coordinating the review of this manuscript and approving it for publication was Norbert Herencsar.

keep track of her general health systems, it is crucial to detect the levels of these hormones [6], [7], [8]. So, the researcher has developed a sensor for sensing the concentration level of hormones in the human body. So far, immunometric assay-based approaches have been employed in the biomedical industry to detect various hormone quantities [9]. However, it has certain drawbacks, including a poor level of sensitivity and accuracy. An optical biosensor is used to create highly sensitive photonic biosensors in order to solve these problems.

The development of novel types of photonic biosensors has received significant research attention to dates such as tumor detection [10], DNA (Deoxyribonucleic acid) sensor [11], support to neural activity [12], and implantable photonic components for medical treatment, etc. Optical fiber-based biosensors also play an important role in the identification of bio components. Bacterial detection [13], glucose in serum [14], cholesterol detection [15], and plasmonic-aided fiber optics sensor [16] are only a few examples. In fiber sensing technology, last few years several authors worked in the Photonic crystal fiber (PCF) based biosensor. Because PCF sensors have numerous advantages for sensing biomedical components such as high sensitivity, low detection limit, compact size, high resolution, and high design flexibility. Further, PCF-based sensors can withstand high voltages, high temperatures, and dangerous chemicals. Due to its many potential uses in non-invasive medical imaging and biological sensing, terahertz frequency is currently the subject of extensive research. Researchers have suggested a variety of guided media for THz propagation during the past few decades, including bare metal wires, metal-coated dielectric tubes, metallic wires, slot waveguides, etc. Yet, the high bending loss, reduced coupling efficiency and maximum material absorption loss of the aforementioned guided mediums force their disregard. The photonic crystal fiber entered the light as a result of innovative light guidance qualities, such as low dispersion, minimum material loss, maximum core power fraction, etc. Recently, many researchers are working on PCF-based biosensors in Terahertz (THz) regime with different structures of the core such as hexagonal, octagonal, elliptical, hollow, and solid cores. Hollow core PCF is more suitable for excellent sensing which is offered strong bonding between light and lower refractive index bio-sample in the core region. Furthermore, PCF offers a precise and efficient detecting capacity in the THz frequency band.

In 2019, Hossain et al. designed a blood sensor using a hollow core for detecting water, plasma, red and white blood cells, and hemoglobin. The obtained maximum relative sensitivity is 93.6% at 2 THz [17]. Further, Kawsar Ahmed et al. have also designed THz based refractive index sensor (RIS) for the detection of blood components using PCF with a sensitivity of 80.56% [18]. Habib et al. designed PCF based cancer detector with high relative sensitivity at 2.8 THz which is 98% [19]. Moreover, Hossain et al. proposed TOPAS based PCF sensor for detecting alcohols with a sensitivity of 86.6% at 1THz [20]. The proposed study has utilized hollow-core PCF in asymmetrical core construction for biosensor application to detect female reproductive hormones by adhering to the same features. Graphene-coated FET (field-effect transistor), is used to monitor parathyroid hormone receptor (PTHR) and G protein-coupled receptor (GPCR), while investigating women's health assessment [21]. In the fiber optic principle, numerous authors reported hormones sensor using tapered optical fiber for dopamine sensor [22], laser detection for thyroid in blood sensor [23], optical fiber-based plasmon nanoparticle endocrine system for controlling body metabolism [24], 1D (one dimensional) Photonic crystal waveguide as women reproductive hormones [25] and plasmon fiber grating [26]. Further, machine learning-based biosensor has been used for many applications that include forecasting, recommendations, recognition, etc. Furthermore, Machine learning algorithms have been vastly employed in photonic devices for the purpose of resource reduction and saving simulation time through the prediction and forecasting of intermediate values [31], [32], [33], [34], [35].

In this article, the asymmetric structure of hollow core PCF is designed for sensing progesterone and estradiol hormones in the THz regime. These hormones work together in every cell and tissue of a woman's body and throughout her life. Further, it is very crucial for reproductive development and sexual in humans. Therefore, a hollow core PCF-based RIS is designed for sensing women's reproductive hormones in order to achieve the healthiness and effective control of the female ovaries based on previously published studies. Further, we have predicted relative sensitivity with help of the Locally Weighted Linear Regression algorithm. The upcoming chapters are showed the proposed sensor design; analyze the sensing performances; and machine learning algorithm for predicting sensor behavior.

II. STRUCTURAL DESIGN

In order to design high relative sensitivity in the THz regime, we have designed rectangular-shaped air holes hollow-core PCF by using the finite element method as depicted in Fig.1. The proposed sensor was designed using the commercially available full vector finite element method (FVFEM) software COMSOL multiphysics v5.3. In order to block stray energy from the fiber axis and absorb radiant light, the perfectly matched layer (PML) thickness is 780 μm. Moreover, the scattering boundary condition is utilized in conjunction with PML to cut down on reflected energy. The cross-section of the sensor is accommodated by a 2D mesh grid made using the finite element technique. Maxwell's equations can be written as a matrix eigenvalue problem to get the imaginary and real effective indices of core modes. We kept the element size extremely fine. The complete mesh consists of 44106 triangular elements, 2180 boundary elements, and 98 vertex elements, and the total mesh area is 506.8 μm^2. The diameter of the optical fiber is 4.85 mm. The rectangular air

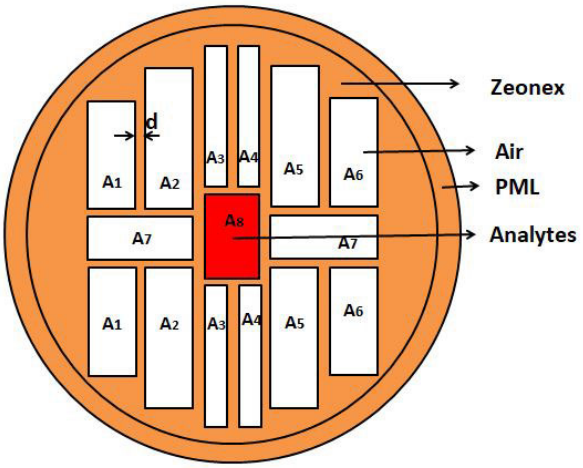

FIGURE 1. Cross section of the THz women reproductive hormones sensor.

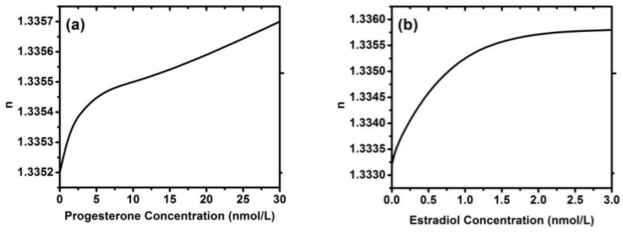

FIGURE 2. RI values of (a) progesterone and (b) estradiol for different concentration levels.

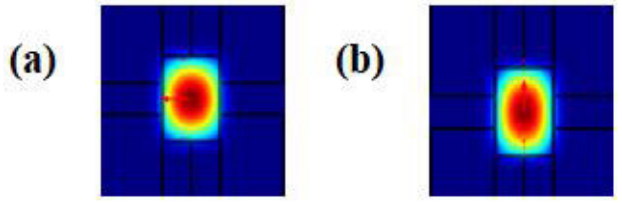

FIGURE 3. Electric field distribution for (a) X- polarization and (b) Y- polarization at 1.35 THz when a progesterone concentration is 10 nmol/L.

holes are considered to surround the core for effective light confinement in the analyte-filling area.

The width and height of A_1, A_2, A_5, and A_6 are equal to 1125 μm and 500 μm, respectively. Similarly, the width and height of A_3 and A_4 are also identical to 1200 μm and 500 μm, respectively. Further, the width and height of A_7 are 250 μm and 1050 μm, respectively. The gap between two rectangular air holes (d) is equal to 10 μm. The background material of the proposed fiber is Zeonex (Refractive Index (RI) = 1.53). It has numerous advantages such as minimum absorption loss, high bio-compatibility, and high-temperature insensitivity compared with other THz materials [27], [28]. Notably, Zeonex and Topas have comparable optical properties, but Zeonex has superior biocompatibility, high glass transition temperature, fabrication flexibility, and maximum chemical resistance than Topas. Although the RI of the backdrop material is closely related to the effective material loss (EML), it also helps to minimize EML in specific grades of Zeonex, such as 330R, 480R, and 480. In this proposed work, we have infiltrated blood samples in the rectangular core region for sensing progesterone and estradiol hormones. The width and height of the rectangular core (A_8) sizes are 450 μm and 690 μm. The simulation makes use of the RI of both hormone concentration levels that were discovered by experimentation. Using a pocket refractometer (Atago PAL-RI), the RI is calculated with respect to different concentrations of progesterone and estradiol in a blood sample as shown in Fig. 2 [25]. The typical range of progesterone and estrogen RI values for women during and after their reproductive years is between 0 and 10 nmol/L and 0 and 3 nmol/L, respectively. As a result, we examined the sensor for reproductive hormones in the range. Further, the proposed asymmetric rectangular PCF can be fabricated with help of 3D printing and extrusion methods which also support the fabrication of complex structures of rectangular air holes [29], [30].

III. RESULTS AND ANALYSIS

Fig. 3 indicates electric field distribution for X- polarization, and Y- polarization at 1.35 THz.

The important parameter of the designed sensor is relative sensitivity which indicates the concentration of sensing analytes. It can be expressed by [27],

$$r = \frac{n_a}{n_{eff}} \times PF \tag{1}$$

where n_a represents the refractive index of an analyte, n_{eff} means effective refractive index, and PF means power fraction in the core region which is expressed by [29],

$$PF = \frac{\int sampleanalytesR_e(E_xH_y - H_xE_y)dxdy}{\int totalR_e(E_xH_y - H_xE_y)dxdy} \tag{2}$$

In order to obtain maximum relative sensitivity, we adjust the structural dimensions. Initially, we considered the distance between two rectangular air holes (d) to be 10 μm and 20 μm. From this optimization, we obtained maximum relative sensitivity at 10 μm due to effective light confinement in the sample region. Fig.4 is shown relative sensitivity for various women's reproductive progesterone hormones with respect to different frequency range at d = 20 μm. From the progesterone hormones, we have obtained maximum relative sensitivity as 97.24% at 1.3 THz for X polarization and 98.43% at 1.35 THz for Y polarization at 10 nmol/L due to maximum refractive index and high power in the core as shown in Fig.4. For estradiol, the maximum sensitivity is 97.26% for X polarization at 1.35 THz and 98.6% at 1.3 THz for Y polarization at 3 n mol/L as shown in Fig.5. A detailed examination of the figures reveals that for X polarization, sensitivity declines after 1.3 THz and for Y polarization, after 1.35 THz. Even though the core power fraction is expected to increase with frequency, it hits its peak at a certain frequency

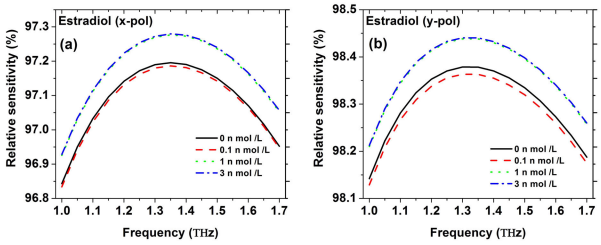

FIGURE 4. Relative sensitivity vs frequency for (a) X-polarization and (b) Y-polarization at d = 20 μm.

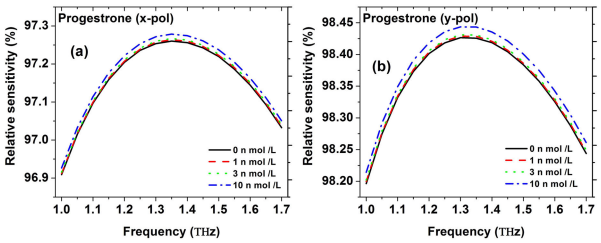

FIGURE 5. Relative sensitivity vs frequency for (a) X-polarization and (b) Y-polarization at d = 20 μm.

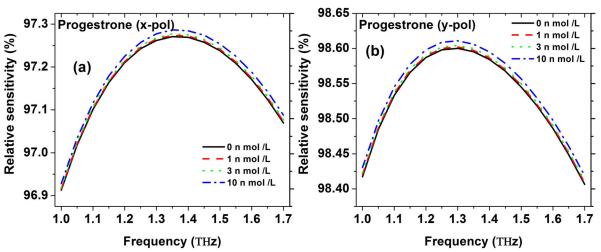

FIGURE 6. Relative sensitivity vs frequency for (a) X-polarization and (b) Y-polarization at d = 10 μm.

and as frequency increases, some useful power begins to leak into the cladding region, causing the core power to weaken.

Further, we have plotted relative sensitivity for d = 10 μm with respect to frequency as shown in Fig. 6 and Fig.7. We have found maximum relative sensitivity as 97.25% at 1.3 THz for X polarization and 98.6% at 1.35 THz for Y polarization at 10 n mol/L as shown in Fig.6. For estradiol, the maximum sensitivity is 97.3% for X polarization at 1.35 THz and 98.63% at 1.3 THz for Y polarization at 3 n mol/L as shown in Fig.7. The obtained relative sensitivity of progesterone and estrogen for different d is shown in Table 1. In the proposed structure, we found the highest relative sensitivity in Y polarization mode, and the reason is the shape of the hollow core maximum in the y direction. And also, it is produced a greater power fraction in the core region. So, we have considered the Y polarization mode for further optimizations.

Then, we increased the hollow core size from the optimum value to +2.5% and decreased it to -2.5%. Fig.8 (a-d) exhibits relative sensitivity for different progesterone concentrations with respect to frequency. The obtained relative sensitivity is

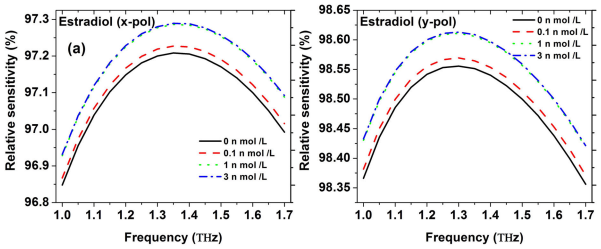

FIGURE 7. Relative sensitivity vs frequency for (a) X-polarization and (b) Y-polarization at d = 10 μm.

TABLE 1. Comparison of relative sensitivity with different values of a gap between rectangular air holes (d).

(d) (μm)	Relative sensitivity (%)			
	Progesterone at 10 nmol/L		Estradiol at 3 nmol/L	
	x-pol at 1.3 THz	y-pol at 1.35 THz	x-pol at 1.3 THz	y-pol at 1.35 THz
20	97.24	98.43	97.25	98.6
10	97.26	98.6	97.3	98.63

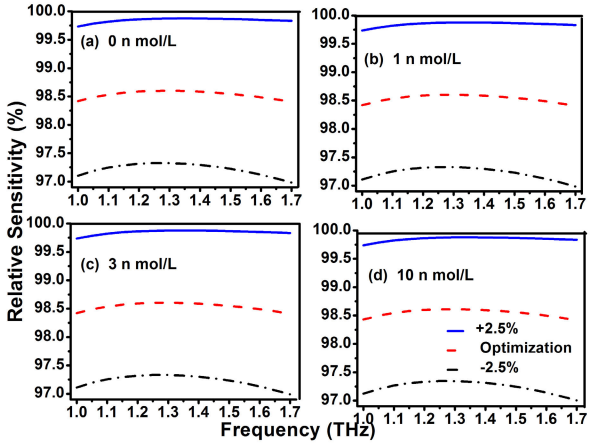

FIGURE 8. Relative sensitivity for Y polarized hollow core optimization when progesterone concentrations are varied.

99.87% for increasing core size and 97.34% for decreasing core size at 1.35 THz. These data are taken at 10 n mol/L as shown in Fig. 8(d). Fig. 8 (a-c) reveals relative sensitivity of 99.81%, 99.83%, and 98.85% at 1.35 THz (increment of 2.5%) for 0 n mol/L, 1 n mol/L, and 3 n mol/L, respectively. Among the four concentrations, the sensitivity is high for 10 n mol/L due to it having a maximum refractive index that causes a more effective light interaction with the analyte.

The maximum relative sensitivity for estradiol hormone is 99.8%, 99.82%, 99.85%, and 99.88% at 1.35 THz (increment of 2.5%) for 0 n mol/L, 0.1 n mol/L, 1 n mol/L, and 3 n mol/L, respectively as shown in Fig. 9 (a-d). The obtained relative sensitivity of progesterone and estradiol for optimization of the analyte filling area is shown in Table 2.

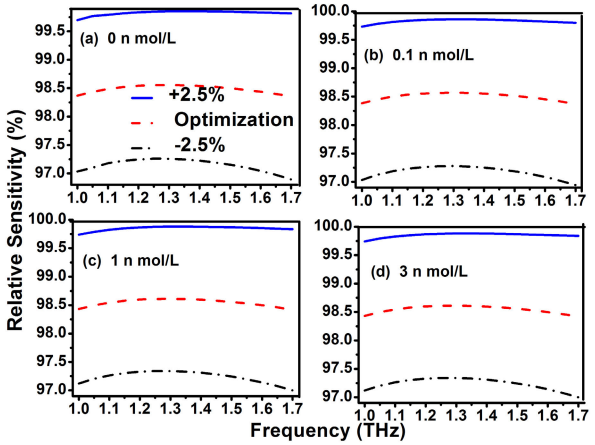

FIGURE 9. Relative sensitivity for Y-polarized hollow core optimization when estradiol concentrations are varied from 0 to 3 nmol/L.

EML is an important parameter for hollow core PCF-based THz sensors which limits the sensing performance. It can by calculated by [27],

$$\alpha_{eff} = \sqrt{\frac{\epsilon_0}{\mu_0}}\left(\sqrt{\frac{J_{max} n_{mat} |E|^2 \alpha_{max} dA}{|\int_{all} S_x dA|}}\right) \tag{3}$$

Where μ_0 and ϵ_0 represent permeability and permittivity in a vacuum, respectively. α_{max} is material absorption loss and n_{mat} is refractive index. E and S_z indicate electric field distribution and pointing vector in the z-direction.

The obtained EML values are plotted with respect to the frequency at the optimized structure as shown in Fig. 10. At minimum frequency, EML value is high for both progesterone and estradiol hormones. When increasing frequency, the interaction of light is very close in the core material which leads to minimum EML. Also, the minimum EML is obtained at a higher refractive index analyte of hormones. The obtained minimum EML values of progesterone hormones are 0.00227 cm^{-1}, 0.00226 cm^{-1}, 0.00225 cm^{-1}, 0.00221 cm^{-1} for 0 nmol/L, 1 nmol/L, 3 nmol/L, and 10 nmol/L, respectively at 1.35 THz. Similarly, estradiol hormones are 0.00247 cm^{-1}, 0.00246 cm^{-1}, 0.00245 cm^{-1}, 0.00242 cm^{-1} for 0 nmol/L, 0.1 nmol/L, 1 nmol/L, and 3 nmol/L, respectively.

Additionally, Fig. 11 depicts the behavior of the proposed core structure's effective mode area in terms of frequency. It can be calculated by [29],

$$A_{eff} = \frac{[\int I(r) r dr]^2}{[\int I^2(r) r dr]^2} \tag{4}$$

where I(r) indicates the transverse electric field intensity.

We found that the effective mode area decreases with an increase in frequency. In addition, the effective area is high at a lower refractive index of hormones due to better light confinement in the core region. The value of effective mode area is noticed as 2.12×10^5 μm^2 (10 n mol/L) for progesterone and 2.34×10^5 μm^2 (0 n mol/L) for estradiol at 1.35 THz frequency. Further, the detection limit (Δn_a) of the proposed THz sensor is 0.0005 and 0.0026 for progesterone and estrogen, respectively.

IV. PREDICTION WITH THE LOCALLY WEIGHTED LINEAR REGRESSION

As it is required to have an optimal structure that can yield high performance and for that simulation is the best way to identify the best-performing structures with optimal parameters. It is more feasible to simulate the structure first and identify the best-performing parameters and for some designs, there would be many parameters to optimize and it would take time for these simulations. Here comes the ML in the picture. ML algorithms can be employed to predict the output for middle wavelengths/frequencies to save simulation time and the simulation can be run for higher step sizes and middle values can be predicted using ML algorithms. This, in turn, will give outputs in lesser time and the optimal structure can also be achieved similarly. Nowadays, Machine learning-based algorithms are vastly applied for the prediction in various photonics devices. Here, a Non-Parametric Learning Method called Locally Weighted Linear Regression (LWLR) will be used. [36], [37]. We'll explore the weighting Function, the predict Function, and finally, visualize the predictions with Python's NumPy and Matplotlib and seaborn libraries. During data training, the ideal value for a parametric algorithm's parameters, such as theta, is sought.

The loss function (J(θ)) for LR is given as:

$$J(\theta) = \Sigma_{i=1}^{m} \left(y^{(i)} - \theta^T x^{(i)}\right)^2 \tag{5}$$

The updated J(θ) for the LWLR is:

$$J(\theta) = \Sigma_{i=1}^{m} w^{(i)} \left(y^{(i)} - \theta^T x^{(i)}\right)^2 \tag{6}$$

where, $w^{(i)}$ is the weight and can be expressed as:

$$w^{(i)} = exp\left(-\frac{(x^{(i)} - x)^T (x^{(i)} - x)}{2}\right) \tag{7}$$

The prediction will be made for x. To designate the i^{th} training exercise is symbolled as $x^{(i)}$. This function's value is bounded by zero and one. Therefore, if we examine the function, we see that when $|x^{(i)} - x|$ is small, the weight is close to 1. With a big value of $|x^{(i)} - x|$, weight is near to 0. Weight is close to 0 for $x^{(i)}$s that are far from x and near to 1 for $x^{(i)}$s close to x. As a result, error terms of J(θ) are multiplied by virtually zero for $x^{(i)}$s very far from x and by almost one for $x^{(i)}$s close to x. The error terms are only added up for the $x^{(i)}$ values somewhat close to x. In order to determine the size of the circle, we incorporate a hyperparameter tau (τ) into the weighting function. Circles' diameters can be made wider or narrower by adjusting the hyperparameter (τ). $w^{(i)}$ now can be written as:

$$w^{(i)} = exp\left(-\frac{(x^{(i)} - x)^T (x^{(i)} - x)}{2\tau^2}\right) \tag{8}$$

TABLE 2. Comparison of relative sensitivity (y-pol) at ±2.5% of analyte filling area with optimum value for 1.35 THz.

	Relative sensitivity (%)							
	Progesterone (n mol/L)				Estradiol (n mol/L)			
	0	1	3	10	0	0.1	1	3
+2.5%	99.81	99.83	99.85	99.87	99.8	99.82	99.85	99.88
Optimum	98.5	98.52	98.55	98.59	98.53	98.56	98.59	98.61
-2.5%	97.21	97.26	97.3	97.34	97.18	97.23	97.27	97.34

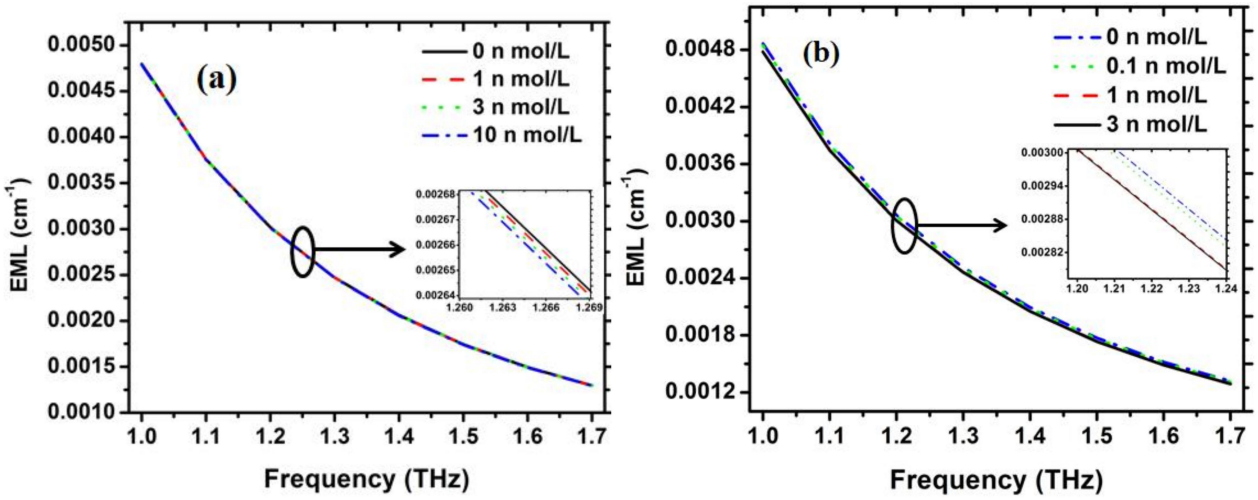

FIGURE 10. EML with respect to frequency of (a) progesterone and (b) estradiol for the optimized proposed structure.

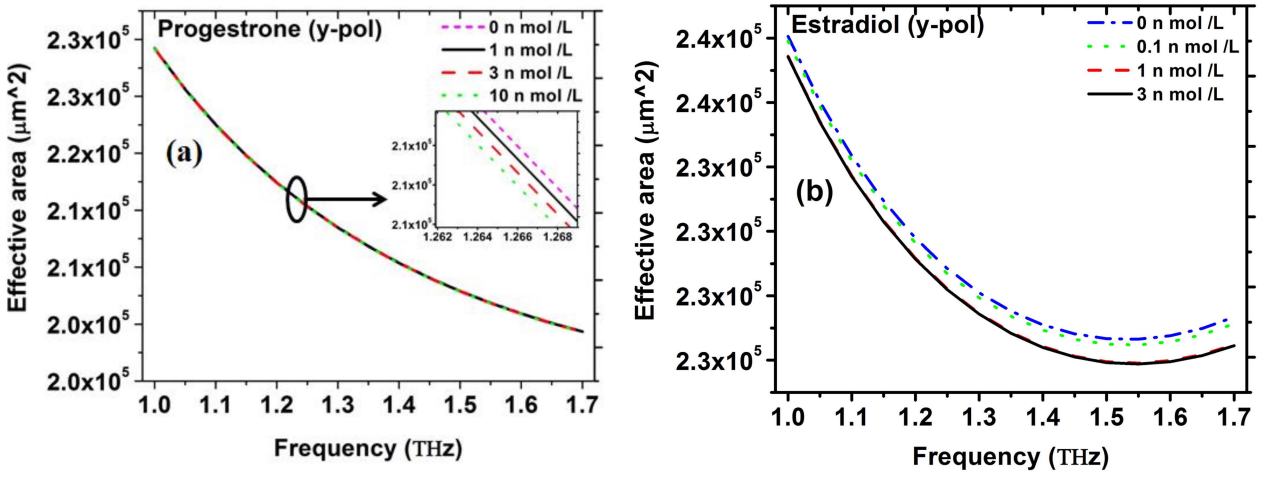

FIGURE 11. Effective mode area with respect to frequency of (a) progesterone and (b) estradiol for the optimized proposed structure.

Theta can also be calculated as:

$$\theta = (X^T WX)^{-1}(X^T WY) \tag{9}$$

Once we have theta, the following expression can be used for predictions:

$$\theta^T x \tag{10}$$

R^2 score, determined in Eq. (11) is used to assess the accuracy of the model.

$$R^2 = 1 - \frac{\Sigma_{i=1}^{N}(PredictedValue_i - ActualValue_i)^2}{\Sigma_{i=1}^{N}(ActualValue_i - AvgValue)^2} \tag{11}$$

The prediction plot derived from this algorithm is presented in Fig. 12 – 14. Fig. 12 demonstrates the actual vs. predicted relative sensitivity values for Progesterone and Estradiol hormones for various concentrations when the distance between consecutive rectangle holes is kept at 20 μm for the weighting hyperparameter value of 0.02. Fig. 12 (a) shows the actual vs. predicted value for Progesterone hormone for the 0 n mol/L concentration and we can see that, after the relative sensitivity of 97.00 it identically fits the actual values. Fig. 12 (b) demonstrates the actual vs. predicted relative sensitivity of Progesterone hormone for the concentration of 10 n mol/L and we can observe that when

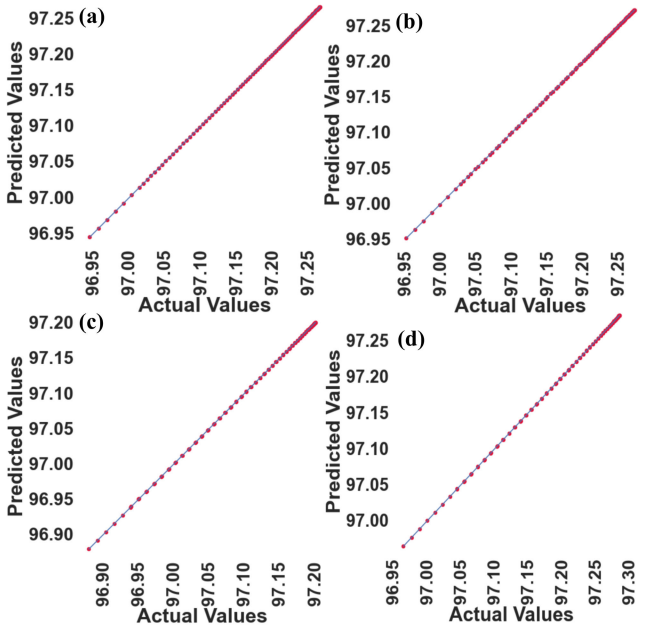

FIGURE 12. Actual vs. predicted values of the relative sensitivity for various hormones with various concentrations for $\tau = 0.02$ and for d = 20 μm (a) Progesterone hormone with the concentration of 0 nmol/L, (b) Progesterone hormone with the concentration of 10 nmol/L, (c) Estradiol hormone with the concentration of 0 nmol/L, (d) Estradiol hormone with the concentration of 3 nmol/L.

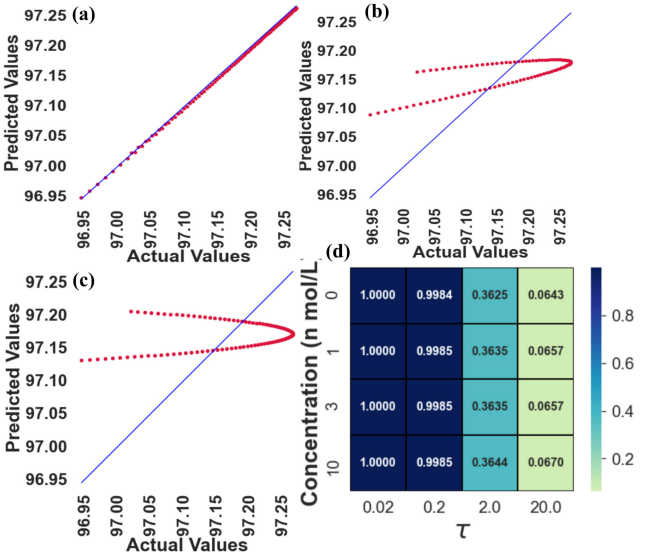

FIGURE 13. Actual vs. predicted values of relative sensitivity for progesterone hormone for the concentration of 0 nmol/L and for d = 20 μm (a) for $\tau = 0.2$, (b) for $\tau = 2$, (c) for $\tau = 20$, (d) Heatmap demonstrating the R2 score for various combination weighing hyper-parameter and various concentration of Progesterone hormone.

relative sensitivity reaches 97.05 the data equivalently fits the actual value. Fig. 12 (c) shows the actual vs. predicted value for Estradiol hormone for the 0 n mol/L concentration and we can see that, after the relative sensitivity of 96.95 it identically fits the actual values. Fig. 12 (d) demonstrates the actual vs. predicted relative sensitivity of Estradiol hormone for the concentration of 3 n mol/L and we can observe that the data equivalently fits the actual value from the beginning.

For the optimization of LWLR, there are several methods and one of the simple ways is to tune the hyperparameters. For the proposed study, τ is the hyperparameter and we have tuned it to optimize the LWLR. And the tuning of hyperparameter, τ has been reported in the manuscript to showcase this. Later, we checked the tuning of the weighting hyper-parameter, τ. For this, we varied the τ in 20, 2, 0.2, 0.02 for both the hormones, and the results are presented in Fig. 13 and 14 separately for the progesterone and estradiol hormones for the concentration of 0 nmol/L. Fig. 13 (a–c) demonstrates the actual vs. predicted values for the progesterone hormone for the $\tau = 0.2$, 2, and 20, respectively. It is quite clear that as we increase the weighting hyper-parameter τ, the prediction accuracy decreases drastically. This behavior is also evidentially clear from the Fig. 13 (d) which demonstrates the R^2 score for progesterone hormone for various concentrations of 0 nmol/L, 1 nmol/L, 3 nmol/L, and 10 nmol/L and weighting hyper-parameter, τ n 20, 2, 0.2, 0.02. It is clear that for $\tau = 0.02$, we achieve the highest R^2 score of 1.0 for all concentrations, and for $\tau = 0.2$, the R^2 score in the range of 0.99 is obtained and later the prediction accuracy drastically decreases for $\tau = 2$ and $\tau = 20$.

TABLE 3. Comparison of various aspects of the proposed PCF to the previous PCF.

Reference	Relative Sensitivity	mode area (μm^2)	Background Material	Frequency (THz)	EML (cm^{-1})
[38]	96	1.5×10^5	Zeonex	1.5	0.0061
[39]	87.68	1.86×10^5	TOPAS	1	-
[18]	80.93	1.8×10^5	TOPAS	1.5	-
[27]	96	7.5×10^4	TOPAS	1.4	0.0035
[40]	85.7	6.9×10^4	Zeonex	1.6	-
Proposed work	99.84	2.21×10^5	Zeonex	1.35	0.0022

Fig. 14 (a–c) illustrates the actual vs. predicted values for the estradiol hormone for $\tau = 0.2$, 2, and 20, respectively. It is evident from the results that as the weighting hyper-parameter is increased, the prediction accuracy decreases substantially. This is also evident from Fig. 14 (d), which depicts the R2 score for the progesterone hormone at different concentrations of 0 nmol/L, 0.1 nmol/L, 1 nmol/L, and 3 nmol/L and weighting hyper-parameter, τ in 20, 2, 0.2, 0.02. It is clear that for τ, we obtain the highest R^2 score of 1.0 for all concentrations; for $\tau = 0.2$, we receive an R^2 score in the vicinity of 0.99; and the prediction accuracy declines severely for $\tau = 2$ and $\tau = 20$.

V. FABRICATION FEASIBILITY OF THE PROPOSED FIBER

The designed hollow-core PCF-based sensor has a few rectangular-shaped air holes, as can be seen in Fig. 1. Today,

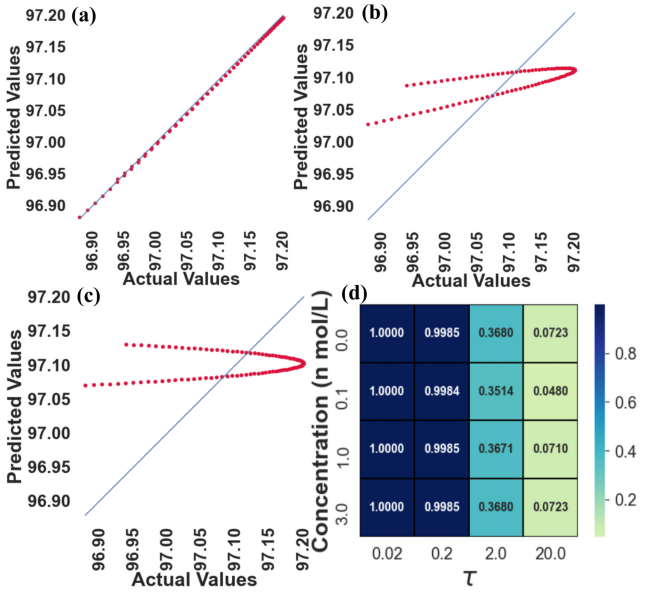

FIGURE 14. Actual vs. predicted values of relative sensitivity for estradiol hormone for the concentration of 0 n mol/L and for d = 20 μm ((a) for $\tau = 0.2$, (b) for $\tau = 2$, (c) for $\tau = 20$, (d) Heatmap demonstrating the R2 score for various combination weighing hyper-parameter and various concentration of estradiol hormone.

capillary stacking, stack and draw, drilling, extrusion, sol-gel, and 3D printing are the most frequently used methods for fabricating PCF [29], [41], [42], [43], [44]. Stack and draw, capillary stacking, and sol-gel techniques are supported to fabricate circular-shaped air hole PCF. Any form of asymmetrical PCF structure can be fabricated by using extrusion and 3D printing technology. The extrusion and drawing by a 3D printer fabrication procedure have been introduced by the National Oceanography Centre, UK, and Optoelectronics Research Centre, UK in order to fabricate suspended structured PCF. The Max Plank Institute, The University Of Adelaide, Australia fabricated several complicated PCF structures using extrusion technology, including rectangular shape air holes and spider-web-shaped PCF [45]. The proposed PCF can be fabricated using the current PCF fabrication technology. Therefore, it is not currently a difficult task to fabricate the proposed rectangular hollow-core PCF.

VI. CONCLUSION

An asymmetric rectangular hollow-core PCF sensor is designed for high detection of progesterone and estradiol hormones in the blood sample at the THz regime (0.8 THz to 1.7 THz). Zeonex is used in the background material for attaining extraordinary sensing properties in the THz region. Using FEM, the numerical sensing performances are evaluated for different concentrations of progesterone and estradiol hormones. The structural parameters such as the strut and core size of the proposed PCF biosensor are optimized to attain maximum relative sensitivity with low loss. The obtained maximum relative sensitivity is 99.87% for 10 n mol/L (progesterone) and 99.88% for 3 n mol/L (Estradiol) at 1.35 THz regime. The Effective material loss (EML) is found around 0.00221 cm^{-1} and 0.00242 cm^{-1} for 10 n mol/L (progesterone) and 3 n mol/L (Estradiol), respectively at 1.35 THz regime. Further, the proposed biosensor offered a large effective area such as 2.12×10^5 um^2 and 2.34×10^5 um^2 for 10 n mol/L (progesterone) and 3 n mol/L (Estradiol), respectively at 1.35 THz regime. Also, this biosensor can be fabricated by current fabrication technologies. The prediction carried out with the help of Locally Weighted Linear Regression, and hyperparameter tuning, we can conclude that for $\tau = 0.02$, the maximum prediction accuracy with the unity R^2 score is observed and this model can be employed for the prediction of relative sensitivity for various parameters.

APPENDIX

See Table 4.

TABLE 4. Abbreviation Table.

PCF	Photonic crystal Fiber
FEM	Finite Element Method
EML	Effective Material Loss
DNA	Deoxyribonucleic acid
THz	Terahertz
GPCR	G protein-coupled receptor
PTHR	Parathyroid hormone receptor
FET	Field-effect transistor
1D	One dimensional
FVFEM	full vector finite element method
RI	Refractive Index

REFERENCES

[1] V. N. Konopsky and E. V. Alieva, "Photonic crystal surface waves for optical biosensors," *Anal. Chem.*, vol. 79, no. 12, pp. 4729–4735, Jun. 2007.
[2] Y. Guo, J. Y. Ye, C. Divin, B. Huang, T. P. Thomas, J. R. Baker Jr., and T. B. Norris, "Real-time biomolecular binding detection using a sensitive photonic crystal biosensor," *Anal. Chem.*, vol. 82, no. 12, pp. 5211–5218, Jun. 2010.
[3] K. V. Sreekanth, S. Sreejith, S. Han, A. Mishra, X. Chen, H. Sun, C. T. Lim, and R. Singh, "Biosensing with the singular phase of an ultrathin metal-dielectric nanophotonic cavity," *Nature Commun.*, vol. 9, no. 1, pp. 1–8, Jan. 2018.
[4] A. B. Hodsman, D. C. Bauer, D. W. Dempster, L. Dian, D. A. Hanley, S. T. Harris, D. L. Kendler, M. R. McClung, P. D. Miller, W. P. Olszynski, E. Orwoll, and C. K. Yuen, "Parathyroid hormone and teriparatide for the treatment of osteoporosis: A review of the evidence and suggested guidelines for its use," *Endocrine Rev.*, vol. 26, no. 5, pp. 688–703, Aug. 2005.
[5] E. Hagstrom, P. Hellman, T. E. Larsson, E. Ingelsson, L. Berglund, J. Sundstrom, H. Melhus, C. Held, L. Lind, K. Michaëlsson, and J. Arnlöv, "Plasma parathyroid hormone and the risk of cardiovascular mortality in the community," *Circulation*, vol. 119, no. 21, pp. 2765–2771, Jun. 2009.
[6] J. C. Prior, "Women's reproductive system as balanced estradiol and progesterone actions—A revolutionary, paradigm-shifting concept in women's health," *Drug Discovery Today, Disease Models*, vol. 32, pp. 31–40, 2020.
[7] J. F. Demayo, B. Zhao, N. Takamoto, and Y. S. Tsai, "Mechanisms of action of estrogen and progesterone," *Ann. New York Acad. Sci.*, vol. 955, pp. 48–59, Mar. 2002.
[8] M. Mihm, S. Gangooly, and S. Muttukrishna, "The normal menstrual cycle in women," *Animal Reproduction Sci.*, vol. 124, nos. 3–4, pp. 229–236, Apr. 2011.
[9] S.-M. Hsu, L. Raine, and H. Fanger, "A comparative study of the peroxidase-antiperoxidase method and an avidin-biotin complex method for studying polypeptide hormones with radioimmunoassay antibodies," *Amer. J. Clin. Pathol.*, vol. 75, no. 5, pp. 734–738, May 1981.

[10] Z. Zeev, A. Rudnitsky, V. Sheinman, A. Tzoy, A. Toktosunov, and A. Adashov, "Home-use cancer detecting band-aid," in *Proc. SPIE*, vol. 9694, 2016, pp. 75–79.
[11] I. S. Amiri, M. M. Ariannejad, J. Ali, and P. Yupapin, "Design of optical splitter using ion-exchange method for DNA bio-sensor," *J. King Saud Univ. Sci.*, vol. 31, no. 4, pp. 549–555, Oct. 2019.
[12] W. Bai, J. Shin, R. Fu, I. Kandela, D. Lu, X. Ni, and Y. Park, "Bioresorbable photonic devices for the spectroscopic characterization of physiological status and neural activity," *Nature Biomed. Eng.*, vol. 3, no. 8, pp. 644–654, Aug. 2019.
[13] R. B. Hayman, "Fiber optic biosensors for bacterial detection," in *Principles of Bacterial Detection: Biosensors, Recognition Receptors and Microsystems*. New York, NY, USA: Springer, 2008, pp. 125–137.
[14] A. M. Hammadi, A. F. Humadi, and A. I. Mahmood, "New optical fiber biosensor method for glucose in serum," *IOP Conf. Mater. Sci. Eng.*, vol. 745, no. 1, 2020, Art. no. 012049.
[15] M. Yunianto, A. N. Permata, D. Eka, D. Ariningrum, S. Wahyuningsih, and A. Marzuki, "Design of a fiber optic biosensor for cholesterol detection in human blood," *IOP Conf. Mater. Sci. Eng.*, vol. 176, no. 1, 2017, Art. no. 012014.
[16] Y. Zhao, R.-J. Tong, F. Xia, and Y. Peng, "Current status of optical fiber biosensor based on surface plasmon resonance," *Biosensors Bioelectron.*, vol. 142, Oct. 2019, Art. no. 111505.
[17] M. B. Hossain and E. Podder, "Design and investigation of PCF-based blood components sensor in terahertz regime," *Appl. Phys. A*, vol. 125, no. 12, pp. 1–8, Dec. 2019.
[18] K. Ahmed, F. Ahmed, S. Roy, B. K. Paul, M. N. Aktar, D. Vigneswaran, and M. S. Islam, "Refractive index-based blood components sensing in terahertz spectrum," *IEEE Sensors J.*, vol. 19, no. 9, pp. 3368–3375, May 2019.
[19] A. Habib, A. N. Z. Rashed, H. M. El-Hageen, and A. M. Alatwi, "Extremely sensitive photonic crystal fiber–based cancer cell detector in the terahertz regime," *Plasmonics*, vol. 16, no. 4, pp. 1297–1306, Aug. 2021.
[20] Md. S. Hossain, N. Hussain, Z. Hossain, Md. S. Zaman, M. N. H. Rangon, Md. Abdullah-Al-Shafi, S. Sen, and M. M. Azad, "Performance analysis of alcohols sensing with optical sensor procedure using circular photonic crystal fiber (C-PCF) in the terahertz regime," *Sens. Bio-Sensing Res.*, vol. 35, Feb. 2022, Art. no. 100469.
[21] S. R. Ahn, J. H. An, S. H. Lee, H. S. Song, J. Jang, and T. H. Park, "Peptide hormone sensors using human hormone receptor-carrying nanovesicles and graphene FETs," *Sci. Rep.*, vol. 10, no. 1, pp. 1–8, Jan. 2020.
[22] N. Agrawal, B. Zhang, C. Saha, C. Kumar, B. K. Kaushik, and S. Kumar, "Development of dopamine sensor using silver nanoparticles and PEG-functionalized tapered optical fiber structure," *IEEE Trans. Biomed. Eng.*, vol. 67, no. 6, pp. 1542–1547, Jun. 2020.
[23] R. Shatti and L. M. H. Al-Ameri, "Optically sensing for thyroid profile hormones in blood," *Medico-Legal Update*, vol. 21, no. 2, pp. 1–5, 2021.
[24] S. K. Srivastava, "SPR based fiber optic sensor for the detection of vitellogenin: An endocrine disruption biomarker in aquatic environments," *Biosensors J.*, vol. 4, no. 1, p. 114, 2015.
[25] N. R. Ramanujam, A. Panda, P. Yupapin, A. Natesan, and P. Prabpal, "Numerical characterization of 1D-photonic crystal waveguide for female reproductive hormones sensing applications," *Phys. B, Condens. Matter*, vol. 639, Aug. 2022, Art. no. 414011.
[26] A. K. Pandey, A. K. Sharma, and C. Marques, "On the application of SiO_2/SiC grating on Ag for high-performance fiber optic plasmonic sensing of cortisol concentration," *Materials*, vol. 13, no. 7, p. 1623, Apr. 2020.
[27] Md. S. Islam, J. Sultana, A. A. Rifat, A. Dinovitser, B. W.-H. Ng, and D. Abbott, "Terahertz sensing in a hollow core photonic crystal fiber," *IEEE Sensors J.*, vol. 18, no. 10, pp. 4073–4080, May 2018.
[28] M. F. H. Arif, K. Ahmed, S. Asaduzzaman, and M. A. K. Azad, "Design and optimization of photonic crystal fiber for liquid sensing applications," *Photonic Sensors*, vol. 6, no. 3, pp. 279–288, Sep. 2016.
[29] H. Ebendorff-Heidepriem, J. Schuppich, A. Dowler, L. Lima-Marques, and T. M. Monro, "3D-printed extrusion dies: A versatile approach to optical material processing," *Opt. Mater. Exp.*, vol. 4, no. 8, pp. 1494–1504, 2014.
[30] T. Yang, C. Ding, R. W. Ziolkowski, and Y. J. Guo, "A terahertz (THz) single-polarization-single-mode (SPSM) photonic crystal fiber (PCF)," *Materials*, vol. 12, no. 15, p. 2442, Jul. 2019.
[31] S. K. Patel, J. Surve, V. Katkar, J. Parmar, F. A. Al-Zahrani, K. Ahmed, and F. M. Bui, "Encoding and tuning of THz metasurface-based refractive index sensor with behavior prediction using XGBoost regressor," *IEEE Access*, vol. 10, pp. 24797–24814, 2022.
[32] S. K. Patel, J. Surve, V. Katkar, and J. Parmar, "Machine learning assisted metamaterial-based reconfigurable antenna for low-cost portable electronic devices," *Sci. Rep.*, vol. 12, no. 1, pp. 1–13, Jul. 2022.
[33] S. K. Patel, J. Surve, V. Katkar, and J. Parmar, "Optimization of metamaterial-based solar energy absorber for enhancing solar thermal energy conversion using artificial intelligence," *Adv. Theory Simulations*, vol. 5, no. 8, Aug. 2022, Art. no. 2200139.
[34] S. K. Patel, J. Surve, J. Parmar, V. Katkar, R. Jadeja, S. A. Taya, and K. Ahmed, "Graphene-based metasurface solar absorber design for the visible and near-infrared region with behavior prediction using polynomial regression," *Optik*, vol. 262, Jul. 2022, Art. no. 169298.
[35] J. Parmar, S. K. Patel, V. Katkar, and A. Natesan, "Graphene-based refractive index sensor using machine learning for detection of mycobacterium tuberculosis bacteria," *IEEE Trans. Nanobiosci.*, vol. 22, no. 1, pp. 92–98, Jan. 2023.
[36] W. S. Cleveland and S. J. Devlin, "Locally weighted regression: An approach to regression analysis by local fitting," *J. Amer. Stat. Assoc.*, vol. 83, no. 403, pp. 596–610, Sep. 1988.
[37] S. K. Patel, J. Surve, J. Parmar, A. Armghan, K. Aliqab, B. R. Altahan, and F. A. Al-Zahrani, "Graphene-based H-shaped biosensor with high sensitivity and optimization using ML-based algorithm," *Alexandria Eng. J.*, vol. 68, pp. 15–28, Apr. 2023.
[38] M. M. A. Eid, M. A. Habib, M. S. Anower, and A. N. Z. Rashed, "Hollow core photonic crystal fiber (PCF)–based optical sensor for blood component detection in terahertz spectrum," *Brazilian J. Phys.*, vol. 51, no. 4, pp. 1017–1025, Aug. 2021.
[39] A. Kumar, P. Verma, and P. Jindal, "Decagonal solid core PCF based refractive index sensor for blood cells detection in terahertz regime," *Opt. Quantum Electron.*, vol. 53, no. 4, pp. 1–13, Apr. 2021.
[40] Md. S. Islam, J. Sultana, K. Ahmed, M. R. Islam, A. Dinovitser, B. W. Ng, and D. Abbott, "A novel approach for spectroscopic chemical identification using photonic crystal fiber in the terahertz regime," *IEEE Sensors J.*, vol. 18, no. 2, pp. 575–582, Jan. 2018.
[41] A. Ghazanfari, W. Li, M. C. Leu, and G. E. Hilmas, "A novel freeform extrusion fabrication process for producing solid ceramic components with uniform layered radiation drying," *Additive Manuf.*, vol. 15, pp. 102–112, May 2017.
[42] R. T. Bise and D. J. Trevor, "Sol-gel derived microstructured fiber: Fabrication and characterization," in *Tech. Dig. Opt. Fiber Commun. Conf. (OFC/NFOEC)*, 2005, p. 3.
[43] W. Talataisong, R. Ismaeel, S. R. Sandoghchi, T. Rutirawut, G. Topley, M. Beresna, and G. Brambilla, "Novel method for manufacturing optical fiber: Extrusion and drawing of microstructured polymer optical fibers from a 3D printer," *Opt. Exp.*, vol. 26, no. 24, p. 32007, Nov. 2018.
[44] Z. Liu, C. Wu, M.-L.-V. Tse, and H.-Y. Tam, "Fabrication, characterization, and sensing applications of a high-birefringence suspended-core fiber," *J. Lightw. Technol.*, vol. 32, no. 11, pp. 2113–2122, Apr. 29, 2014.
[45] S. Atakaramians, S. Afshar, H. Ebendorff-Heidepriem, M. Nagel, B. M. Fischer, D. Abbott, and T. M. Monro, "THz porous fibers: Design, fabrication and experimental characterization," *Opt. Exp.*, vol. 17, no. 16, p. 14053, Aug. 2009.

A. NAESHA NITHISH received the B.E. degree in electronics and communication engineering from the Thiagarajar College of Engineering, Madurai, Tamil Nadu, India, in 2022. He is currently with Deloitte USI, Bengaluru, Karnataka.

SHOBHIT K. PATEL (Senior Member, IEEE) received the Ph.D. degree in electronics and communication engineering from the Charotar University of Science and Technology, Changa, India. He is currently working in the areas of photonics, metamaterial, antenna, optics, and artificial intelligence. He has published several research articles in high-impact SCI journals. He has also filed seven Indian patents on different novel research done by him. He received DST International Travel Grant, in 2014, to present a paper at the IEEE APS-URSI Symposium in Memphis, USA. He also received the DST International Travel Grant, in 2017, to present a paper at the PIERS Symposium, NTU, Singapore. He was named in the list of "top 2% scientists worldwide identified by Stanford University," in 2021. He is currently working on many graphene-based projects and has received funding from SERB and DST, for his research. He has been honored with awards for his achievements in the area of research field.

N. AYYANAR received the B.E. degree in electronics and communication from the Narasu's Sarathy Institute of Technology, Salem, India, in 2013, the M.E. degree in optical communication from the Alagappa Chettiar Government College of Engineering and Technology, Karaikudi, India, in 2015, and the Ph.D. degree in electronics and communication engineering from the National Institute of Technology, Tiruchirappalli, India, in 2020. He is currently an Assistant Professor with the Department of Electronics and Communication Engineering, Thiagarajar College of Engineering, Madurai, Tamil Nadu, India. He has published 27 articles in refereed international journals and over 21 papers at conferences. His research interests include PCF-based optical fiber sensors, few-mode fibers, fiber laser, plasmonics, and few-mode amplifier system designs.

JAYMIT SURVE (Graduate Student Member, IEEE) received the B.Tech. degree in electrical engineering from the Institute of Infrastructure Technology Research and Management, Ahmedabad, and the M.E. degree in electrical engineering with specialization in automatic control and robotics from The Maharaja Sayajirao University of Baroda, Vadodara. He joined Marwadi University as a Junior Research Fellow, in July 2021. His recent research interests include multidisciplinary research in the field of absorbers, sensors, graphene, robotics, and AI-based disaster management for search and rescue missions.

S. RAJARAM (Senior Member, IEEE) received the B.E. degree in electronics and communication from the Thiagarajar College of Engineering, Madurai, Tamil Nadu, India, in 1994, the M.E. degree in microwave and optical engineering from the Alagappa Chettiar Government College of Engineering and Technology, Karaikudi, India, in 1996, and the Ph.D. degree in VLSI design from the Thiagarajar College of Engineering, in 2008. He was a Postdoctoral Research Fellow (BOYSCAST Fellow) in 3-D wireless system design with the Georgia Institute of Technology, Atlanta, USA, from August 2010 to July 2011. He is currently a Professor with the Department of Electronics and Communication Engineering, Thiagarajar College of Engineering. He has published 76 articles in refereed international journals and over 103 papers in conferences. His research interests include optical, microwave, VLSI, wireless communication, wi-max, medical imaging, and artificial intelligence.

S. N. DEEPA is currently an Associate Professor in electrical engineering with the National Institute of Technology Arunachal Pradesh, Jote, Arunachal Pradesh. She possesses 18 years of teaching and research experience and has published ten books with national/international publishers, 106 international journal articles, 12 national journal articles, and 53 papers at national/international conferences. Her research interests include linear and non-linear control system design and analysis, soft computing techniques, evolutionary strategies, adaptive and robust control systems, and medical image processing techniques. She is recognized in the Top 2% of the world's scientist list ranked by Stanford University, USA. With respect to her research attributes, she possesses 9174 citations, Google Scholar H-index of 22 and an i10-index of 58, her Scopus H-index is 16, and the Web of Science H-index is 12 as on date. Her research gateway score is 28.43.

TRUONG KHANG NGUYEN (Senior Member, IEEE) received the B.S. degree in computational physics from the University of Science, Vietnam National University, Ho Chi Minh City, Vietnam, in 2006, and the M.S. and Ph.D. degrees in electrical and computer engineering from Ajou University, Suwon, South Korea, in 2013. From October 2013 to December 2014, he was with the Division of Energy Systems Research, Ajou University, as a Postdoctoral Fellow. He is currently the Head of Division of Computer Engineering, Faculty of Information Technology, School of Technology, Van Lang University, Ho Chi Minh city. He has authored or coauthored 70 peer-reviewed ISI journal articles and 40 conference papers. He has written one book chapter in the area of terahertz antenna and led one patent on terahertz stripline antenna. His current research interests include microwave antenna for wireless communication, terahertz antenna for compact and efficient sources, and nanostructures and nanoantenna for optical applications.

FAHAD AHMED AL-ZAHRANI received the B.Sc. degree in electrical and computer engineering from Umm Al-Qura University, Makkah, Saudi Arabia, in 1996, the M.S. degree in computer engineering from the Florida Institute of Technology, in 2000, and the Ph.D. degree in computer engineering from Colorado State University, in 2005. He is currently a Professor with the Computer Engineering Department, Umm Al-Qura University. He has taught several computer network courses and supervised related research projects. From 2011 to 2016, he was the IT Dean of Umm Al-Qura University and has had several other responsibilities. His research interests include high-speed network protocols, sensor networks, optical networks, performance evaluation, the IoT, blockchain architecture, and performance analysis. He is a member of the International Society for Optical Engineering and the Optical Society of America.